SAND2011-5353C

Evaluation of a New Tool for Heliostat Field Flux Mapping

Clifford K. Ho[1], Siri S. Khalsa[2], David Gill[1], and Cianan A. Sims[1]

[1]Sandia National Laboratories, Concentrating Solar Technologies Department, P.O. Box 5800, Albuquerque, NM 87185-1127, USA, (505) 844-2384, ckho@sandia.gov

[2]Sandia Staffing Alliance, P.O. Box 5800, Albuquerque, NM 87185-1127, USA

Abstract

A method for calculating the irradiance distribution on a receiver or target is further evaluated in this paper. The method, called PHLUX (Photographic Flux) mapping, uses a CCD camera to determine the irradiance distribution using recorded images of the illuminated receiver or target. The only information that is required is the direct normal irradiance, the receiver reflectivity, the subtended source angle of the sun (~9.3 mrad), and the pixel values of the receiver and sun images. Additional sensors, flux gauges, calorimeters, or scaling factors are not required. The novel feature of this method is that an image of the sun is used to scale both the magnitude and subtended angle of each pixel. This paper describes tests to evaluate the impact of camera settings (shutter speed, aperture, and filters) on the CCD response. Additional tests are performed that demonstrate that the FLUX method is independent of distance and angle between the camera and target, and that the method can be applied to non-planar (tubular) surfaces. Finally, the method is applied to estimate the irradiance on the PS10 receiver.

1. Introduction

A new method to determine irradiance distributions on central receivers and targets from heliostats or other collectors for concentrating solar power applications has been recently introduced [1]. The method uses a CCD camera, and, unlike previous beam characterization systems [2]-[7], it does not require additional sensors, calorimeters, flux gauges, mechanical wands, or estimations of heat loss from the receiver or target. In addition, spillage can exist (the beam does not need to be contained within the target). The only additional information required besides the digital images recorded from the CCD camera is the direct normal irradiance and the reflectivity of the receiver. Methods have been described to calculate either an average reflectivity or a reflectivity distribution for the receiver using the CCD camera, and previous results showed that this method (called PHLUX – Photographic Flux mapping) was capable of producing an accurate flux map of a heliostat beam with a relative error in the peak flux of 2%. [1]. The novel feature of this new PHLUX method is the use of recorded images of the sun to scale both the magnitude of each pixel value and the subtended angle of each pixel.

This paper provides additional evaluations of the PHLUX tool, including an assessment of the linearity and accuracy of camera response (including neutral-density filter attenuation), a test of the independence of camera position on irradiance measurements, and the impact of tubular geometries on irradiance measurements. In addition, the PHLUX method was applied to images of the cavity receiver of the PS-10 direct-steam generation power tower near Seville, Spain.

2. Approach

The camera response and linearity were tested on a Canon 350D and Nikon D90. Images of the sun were taken at different shutter speeds and f-stops (aperture openings) to determine the impact of different settings on the response of the CCD (charge coupled device). In addition, different neutral density filters, which are used to prevent saturation of the CCD pixels, were applied to determine the accuracy of the manufacturer provided optical density (attenuation factor).

Another test was performed to evaluate the effect of camera position (varying distances and angles) on

irradiance measurements of a facet beam on a diffuse target. In theory, the irradiance measurements are independent of camera position [1]. In addition, irradiance measurements were made on tubular receivers to investigate the impact of a more complex surface geometry (with peaks and valleys). Finally, during a tour of PS10/20, photographs of the cavity receiver were taken and processed using the PHLUX method to estimate irradiance distributions within the cavity.

3. Results and Discussion

3.1. Camera Settings and Linearity

The Canon 350D and Nikon D90 were evaluated to determine the impact of aperture, shutter speed, and filter attenuation on the pixel values that are used in the PHLUX method. Images of the sun were taken with a variety of apertures, shutter speeds, and neutral-density filters (to prevent pixel saturation). Tests with the Canon 350D revealed that its CCD response was approximately linear with respect to shutter speed. Figure 1 shows the cumulative pixel value (green channel) as a function of shutter setting and shutter speed.

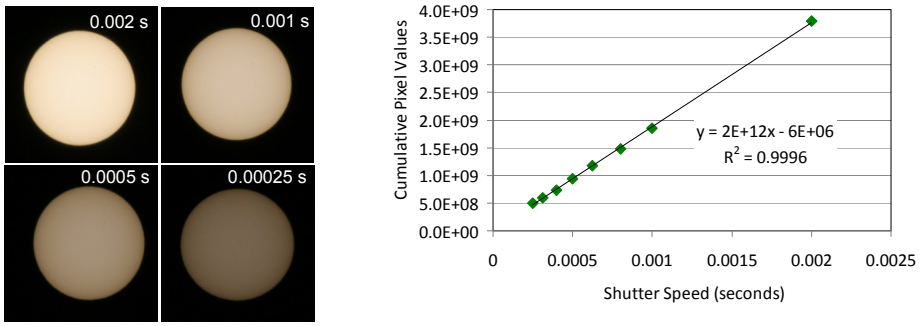

Figure 1. Images of the sun (left) and response of the Canon 350D (right) as a function of shutter speed.

Tests with both the Canon 350D and the Nikon D90 were performed to investigate the impact of filter attenuation and aperture area, where the aperture area is equal to $\pi(f/(2N)^2$, f is the focal length, and N is the f-number. The left plot in Figure 2 shows that the average CCD pixel value (red, green, and blue) is linearly proportional to the aperture area (and hence power hitting the CCD) for a given filter attenuation. The focal length was held constant at 300 m and the f-number was varied from f16 to f32 during quick successive photos of the sun on a clear day. The right plot in Figure 2 shows the impact of neutral density filters on the recorded pixel values. The actual filter attenuation factor is calculated as the inverse of the ratio of the average pixel values with and without a prescribed set of neutral density filters when quick successive photos of the sun were taken. The theoretical filter attenuation is calculated as 10^d, where d is the optical density of the filter (d=0.3 yields a theoretical attenuation of 2, and d=0.9 yields a theoretical attenuation of 7.94). Results show that the actual attenuation can be quite different than the theoretical attenuation, depending on which channel is used. In addition, the red channel exhibits a non-linear behavior with increasing filter attenuation. Therefore, this study recommends that, when possible, the same camera settings and filters be used between images of the receiver and sun (for calibration) so that any errors associated with different settings and filters are negated. When different filters are needed, the pixel values from the green channel should be used (for both filter characterization and processing).

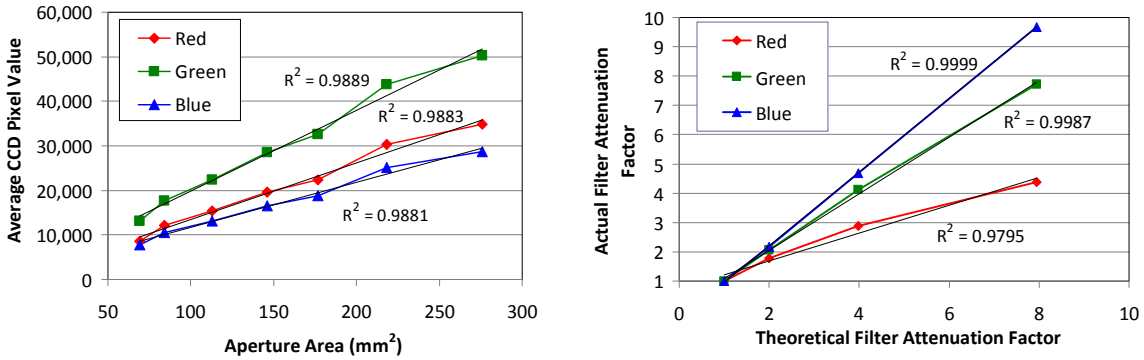

Figure 2. Evaluation of CCD linearity (left) and impact of ND filter attenuation (right) for the Nikon D90 camera.

3.2. Distance and Angle Independence

A single mirror facet (focal length ~4 m) was used to project a beam of sunlight onto a Duraboard HD target. Photographs of the beam were taken at different angles and distances relative to the target to confirm that the angle and distance between the camera and target should not have any impact on the pixel values and, hence, predicted irradiance, as predicted by theory [1]. Figure 3 shows photos of the test and a sketch of the approximate locations where the photographs were taken relative to the target. Results showed that the coefficient of variation (standard deviation divided by the mean) of the average pixel value within the beam at all angles and distances was only 2.4%. This was similar to the variability of the direct normal irradiance (DNI) during the test, which varied between 1000 – 1020 W/m^2. Thus, these tests confirm that the PHLUX method does not depend on the angle or distance between the camera and target to estimate the irradiance on a diffuse target from reflected images.

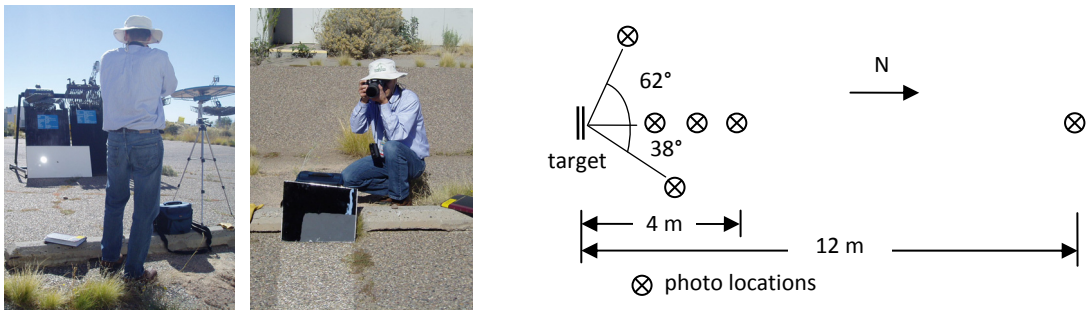

Figure 3. Single-facet beam evaluation at different angles and distances.

3.3. Non-Planar Receiver Surfaces

The derivation of the PHLUX method in Ho and Khalsa [1] showed that the calculated irradiance on a receiver was dependent only on the DNI, reflectivity of the diffuse receiver, subtended sun angle, and recorded pixel values of images of the receiver and sun. The irradiance did not depend on the angle or distance between the camera and receiver (as demonstrated in Section 3.2), nor on the surface geometry. In order to test the PHLUX method's independence from surface geometry, tests were conducted by projecting beams from a single facet onto tubular receivers (Figure 4). The accuracy of the irradiance distribution on a tubular surface calculated by the PHLUX method was assessed by comparing the estimated irradiance with the irradiance from the same beam on a planar surface at the same location. Because of the variable surface topology (peaks and valleys) of the tubular panel, a beam on the tubular surface yielded measured irradiances with bands of lower irradiance in the valleys (clefts) of the tubular panel (Figure 4). The effective surface area is greater in the valleys (where the sides of the tubes meet) than along the peaks, where the top of each

tube is exposed. For a given incident power on the receiver, regions with greater area yield lower irradiance values. A derivation is presented in the Appendix to map the irradiance from a planar surface to a tubular surface.

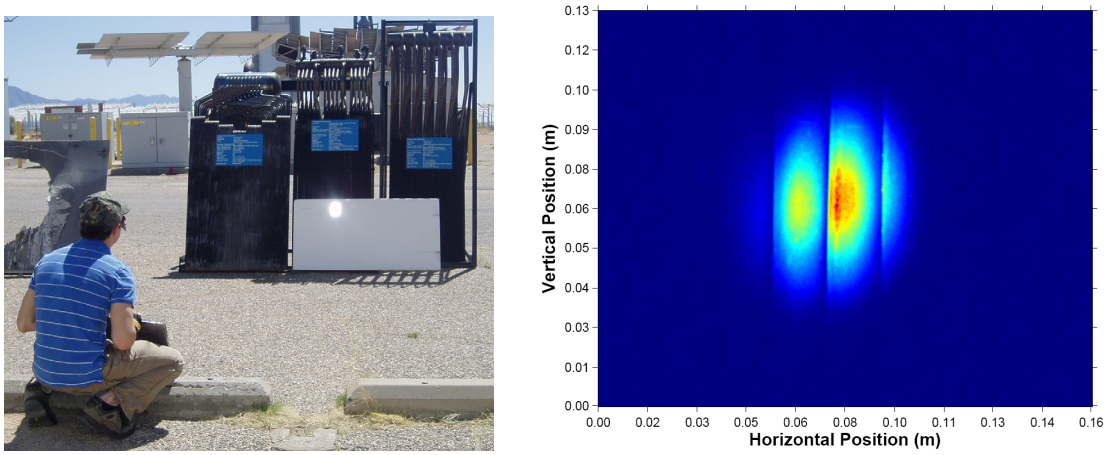

Figure 4. Left: Projecting a beam from a focused facet onto both a flat Duraboard HD target and a tubular receiver display. Right: PHLUX map of beam on tubular receiver.

The plots shown in Figure 5 are used to validate the irradiance profile yielded by a photograph of a beam on a tubular receiver. First, a photograph was taken of a beam focused onto a flat panel of Duraboard HD using a single focusing facet (see Figure 4). The expected irradiance distribution on the tubular receiver from this same beam can be predicted using Eq. (6) in the Appendix. The function I(x) in Eq. (6) is obtained from the photograph of the beam on the flat sheet. Second, the same mirror was reoriented to shift the beam slightly upward onto the tubular receiver on which the Duraboard HD was leaning. The normalized irradiance yielded by the photograph of the beam on the tubular receiver is compared to the predictions of Eq. (6) in the plots below. The irradiance profile of the beam on the flat panel is also plotted for reference in Figure 5. Results show that the measured irradiance distribution on the tubular receiver is similar to the measured irradiance distribution on the flat panel except for local regions of reduced irradiance caused by the increased surface area of the clefts in between the tubes. The theoretical mapping of the irradiance from the flat panel onto the tubular surface matches the general trend of the measured irradiance distribution on the tubular surface for conditions when the beam was centered near a cleft and when the beam was centered near a tubular peak. This provides additional confidence that the PHLUX method is able to calculate the irradiance distribution on non-planar surfaces. It should be noted that local variations in reflectivity of the target surfaces can cause variations in the PHLUX-measured irradiance, but in this test, the reflectivity-induced variations are small relative to the overall trends in the distributions. Ho and Khalsa [1] describe methods for calculating a reflectivity map for the target surface using the PHLUX method.

Some methods of creating a receiver flux map rely on using a scaling factor to scale each pixel value of the illuminated receiver image to an irradiance value. The scaling factor is determined from an image of the receiver illuminated by a beam of known power, say, from a single heliostat, that is completely contained on the receiver. This scale-to-known-power method requires an area-per-pixel conversion factor for every pixel illuminated by the beam. The reason is that for a diffuse surface, no matter what the camera distance or viewing angle, a CCD-value is proportional to the irradiance (power per unit area) on the corresponding region of the receiver and not the total power received by that receiver region. This claim is supported by the PHLUX derivation [1] as well as the distance- and angle-independence testing described in Section 3.2. Therefore, in order to scale to a power, the receiver area corresponding to each pixel must be known. For a general non-planar geometry, this area-per-pixel conversion factor can be unique to every pixel. When using this scale-to-known-power method, if the user does not use knowledge of the receiver geometry to calculate a unique area-per-pixel conversion factor for each pixel illuminated by the beam, then the resulting scaling factor will be incorrect.

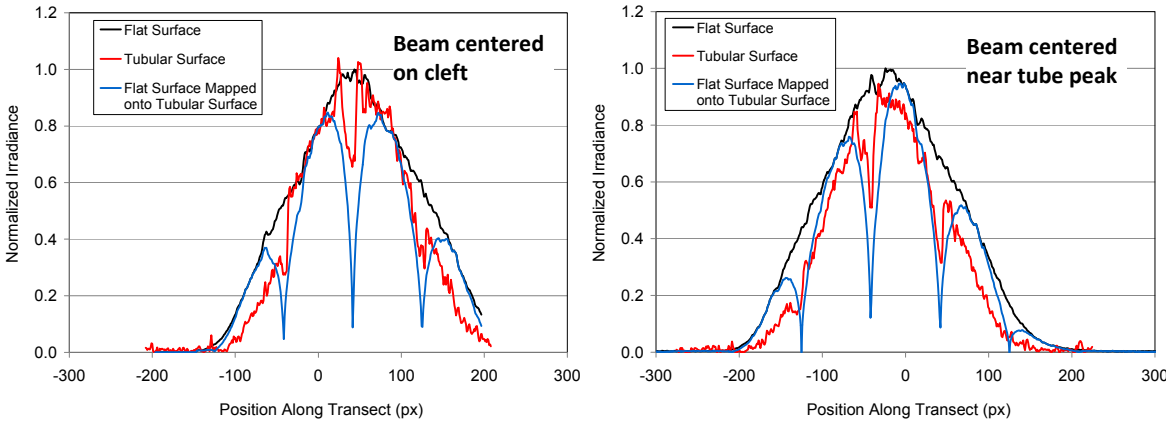

Figure 5. PHLUX-calculated normalized irradiance distributions from the same projected beam on a flat surface and on a tubular surface, along with a theoretical mapping of the irradiance from the flat surface onto a tubular surface. Left: beam centered near cleft of tubes. Right: beam centered near peak of tubes.

3.4. Application to PS10 Cavity Receiver

The PHLUX method was applied to images taken of the PS10 cavity receiver during a tour of the facility. Figure 6 shows photographs of the receiver and the resulting irradiance distribution calculated using the PHLUX method with an assumed average reflectivity of 0.05. Results show that the measured irradiance distribution in the image ranged from ~200 – 500 kW/m^2, which corresponds to the range of irradiance values reported by sensors within the receiver at the time the photograph was taken. The vertical and horizontal distances on the PHLUX map were estimated using the subtended angle of the sun as a scaling factor together with an estimate for the distance between the camera location and the tower (~350 m) and the height of the receiver (~110 m). Uncertainty in these distances will only affect the scaling of the vertical and horizontal distances on the PHLUX map, not the irradiance values. Discrete "bright" spots in the PHLUX map indicate regions on the receiver where the reflectivity was significantly higher than the rest of the receiver (i.e., where the black paint was worn off), indicating a need for determination of a spatially varying map of the reflectivity of the receiver to resolve the irradiance in those regions. Ho and Khalsa [1] provide a simple method to determine the reflectivity distribution.

3.5. PHLUX Web Tool

We have developed a web-based PHLUX tool that can be used to evaluate the irradiance on receivers and targets. Photographs of the illuminated receiver can be uploaded together with images of the sun. Drawing tools allow the user to select regions of interest, and relevant data can be entered (e.g., DNI, reflectivity). Output from the PHLUX web tool includes data and plots of the irradiance distributions. Figure 7 shows screen images of the web-based PHLUX tool. The URL for the website is www.sandia.gov/phlux.

4. Conclusions

This paper has provided additional evaluations of the PHLUX method, which was first described by Ho and Khalsa [1]. The PHLUX method allows a user to determine an irradiance profile on a receiver or target with arbitrary geometry using a standard digital camera, without any knowledge of the receiver geometry, target distance, or viewing angle. This is assuming the user knows the reflectivity of the receiver. The only information that is required is the DNI, target reflectivity, subtended sun angle (~9.3 mrad), and the recorded pixel values of the receiver and the sun images.

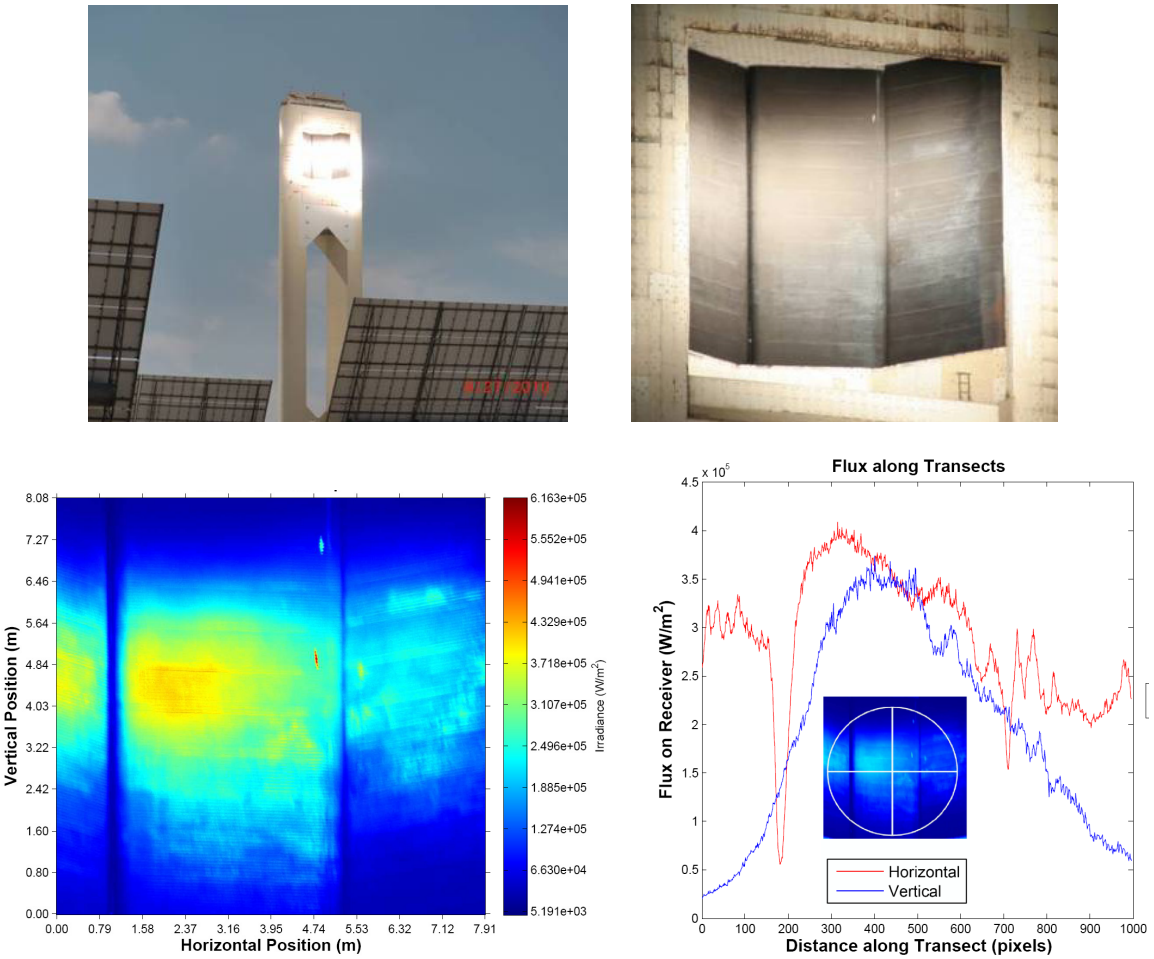

Figure 6. Photographs of illuminated PS10 receiver (top) and PHLUX-calculated irradiance distributions (bottom) within the cavity receiver (~13:00, September 27, 2010, DNI ~ 800 W/m^2).

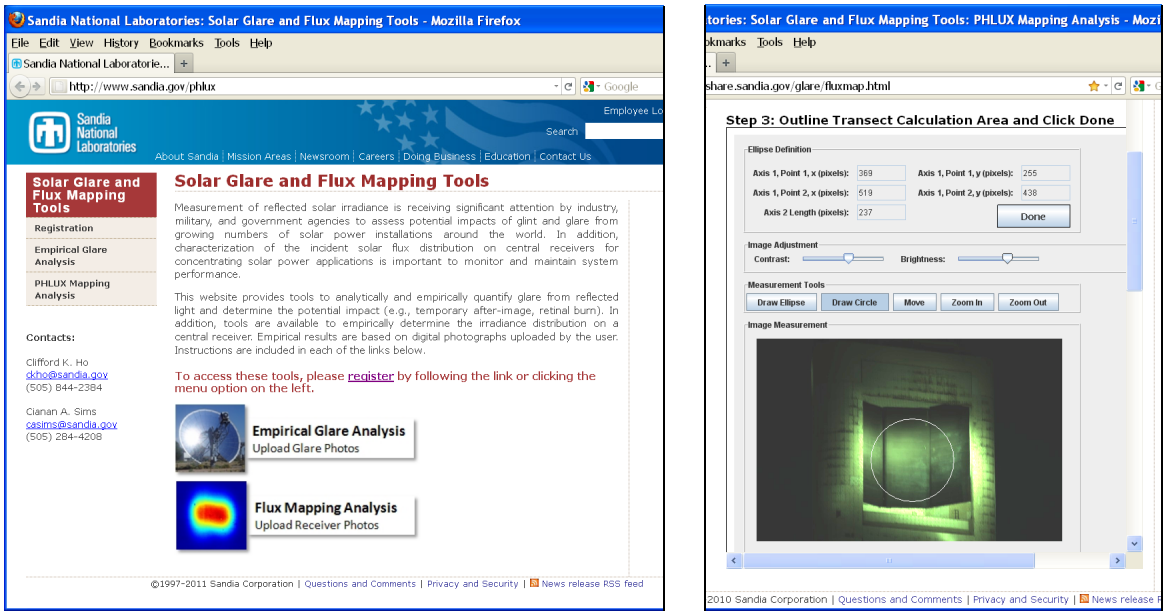

Figure 7. Screen images of the web-based PHLUX tool.

This study evaluated the impact of camera settings (shutter speed, aperture, and filters) on the PHLUX method. Results showed that the CCD response for both the Canon 350D and the Nikon D90 cameras was linear with respect shutter speed and aperture. Variations in the actual attenuation relative to the theoretical attenuation factor of neutral density filters were significant. For the Nikon D90, the green channel exhibited the most linear and representative response for different attenuation factors. Tests were performed that demonstrated that the PHLUX method was independent of distance and angle between the camera and target. In addition, tests showed that the PHLUX method could be used on non-planar (tubular) surfaces as well as flat surfaces.

Finally, the PHLUX method was applied to images taken of the interior of the PS10 receiver during a tour of the facility. Results showed that the calculated irradiance distribution using the images was similar to the irradiance measured from flux gauges installed within the receiver.

Acknowledgments

Sandia National Laboratories is a multi-program laboratory managed and operated by Sandia Corporation, a wholly owned subsidiary of Lockheed Martin Corporation, for the U.S. Department of Energy's National Nuclear Security Administration under contract DE-AC04-94AL85000.

References

[1] Ho, C.K. and S.S. Khalsa, 2011, A Flux Mapping Method for Central Receiver Systems, in proceedings of the 2011 ASME Energy Sustainability Conference, Washington D.C., August 7-10, 2011.

[2] Mavis, C.L., 1988, "10 MWe Solar Thermal Central Receiver Pilot Plant Heliostat and Beam Characterization System Evaluation November 1981 – December 1986," SAND87-8003, Sandia National Laboratories, Livermore CA.

[3] Blackmon, J.B., 1985, "Development and performance of a digital image radiometer for heliostat evaluation at Solar One, J. Solar Energy Engr., 107, 315-321.

[4] Ulmer, S., W. Reinalter, P. Heller, E. Lupfert, and D. Martinez, 2002, Beam Characterization and Improvement with a Flux Mapping System for Dish Concentrators, J. Solar Energy Engr., 124, 182-188.

[5] Yogev, O., P. Gleckman, and M. Rozler, 2009, "High-Heat Solar Flux Scanner," in proceedings of SolarPACES 2009, Berlin, Germany, September 15-18, 2009.

[6] Naor, G., G. Goldwine, R. Hayut, O. Bibi, E. Silberstein, O. Chernin, Z. Auman, G. Kroyzer, and A. Ziskin, 2010, "Flux Measurement System Using IR Camera," in proceedings of SolarPACES 2010, Perpignan, France, September 21-24, 2010.

[7] Slack, M., P. Meduri, and A. Sonn, 2010, "eSolar Power Tower Performance Modeling and Experimental Validation," in proceedings of SolarPACES 2010, Perpignan, France, September 21-24, 2010.

Appendix: Theoretical Mapping of Irradiance from a Flat Surface to a Tubular Surface

Consider one tube of a tubular receiver exposed to some directional incident radiative flux $\vec{\mathbf{I}}(x)$ [W/m^2], as illustrated Figure 8, with an infinitesimal area dA [m^2] located at point (x, y) on the tube surface. Any radiation that strikes dA must have passed through the area $\mathrm{d}\vec{\mathbf{a}}$ [m^2], whose normal is aligned with $\vec{\mathbf{I}}(x)$. Therefore, the power, p [W], that strikes dA is given by:

$$p = \vec{\mathbf{I}}(x) \cdot \mathrm{d}\vec{\mathbf{a}} = \mathrm{I}(x) \cdot \mathrm{da} \tag{1}$$

The local irradiance, E [W/m^2] intercepted by dA is given by:

$$E(x) = \frac{p}{\mathrm{dA}} = \frac{\mathrm{I}(x) \cdot \mathrm{da}}{\mathrm{dA}} \tag{2}$$

By definition, da is given in terms of dA by:

$$da = dA \sin\theta' = \frac{dA}{\sqrt{1+\frac{1}{\tan^2\theta'}}} \tag{3}$$

which yields the following for the local irradiance on the tubular surface:

$$E(x) = \frac{I(x)}{\sqrt{1+\frac{1}{\tan^2\theta'}}} \tag{4}$$

If the irradiance is perpendicular to the overall plane of the receiver, $\theta' = \theta$, which yields:

$$\tan^2\theta' = \frac{y^2}{x^2} = \frac{r^2 - x^2}{x^2} \tag{5}$$

Substituting (3) and (5) in (2) yields the following equation for the local irradiance on the tube:

$$E(x) = I(x)\sqrt{1-\frac{x^2}{r^2}} \tag{6}$$

where I(x) is obtained from the irradiance on a flat surface and x=0 corresponds to the peak of the tube. As an illustration, suppose the irradiance function, I(x), on a flat surface is Gaussian with a standard deviation equal to one tube diameter. The transformed irradiance distribution on a tubular surface consisting of seven adjacent tubes using Eq. (6) is plotted in Figure 8. It should be noted that deviations of the direction of the incident radiative flux away from the normal to the surface, as assumed here, could cause errors in the calculated theoretical irradiance distribution on a tubular surface mapped from a planar surface.

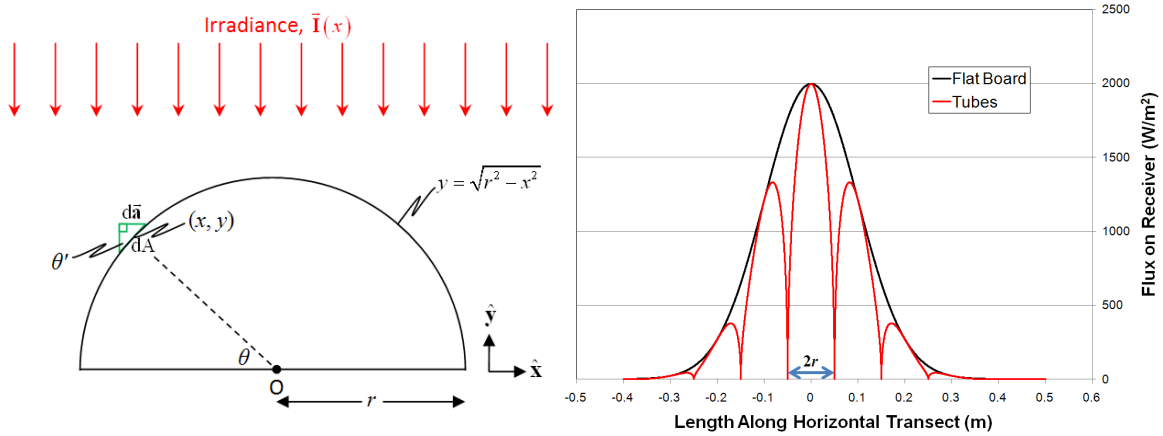

Figure 8. Schematic of irradiance onto a single tube (left). Plot of irradiance on a flat surface and a surface composed of seven adjacent tubes assuming a Gaussian irradiance distribution.